ON MOISTURE INDUCED PROPETRY CHANGES AND STRESS ANALYSIS OF A SINGLE FIBER COMPOSITE DURING AGEING

M. Lai, J. Botsis, D. Coric and J. Cugnoni
Laboratoire de Mécanique Appliquée et d'Analyse de Fiabilité (LMAF)
École Polytechnique Fédérale de Lausanne (EPFL), CH-1015 Lausanne, Switzerland
marco.lai @epfl.ch

SUMMARY

The hygrothermal response of an epoxy is reported as function of average moisture uptake. The specimen used is a single fibre composite with axially located optical fibre that contains a Bragg grating sensor. Bragg grating strain data are compared with stress analysis accounting for moisture diffusion in the specimen.

Keywords: Moisture, visco-elasticity, single fibre composite, fibre Bragg grating sensors, material testing.

INTRODUCTION

Service life extension of aerospace and automotive composite components imposes the need for a better understanding of ageing of these structures. Moisture absorption, for instance, is recognized to be one of the most important causes in impairing polymer mechanical properties since it induces physical changes at a microscopic level.
The water influence on polymers has been addressed widely in the past by several authors. Zhou and Lucas [1] clearly assessed the nature of the absorbed water by means of solid state NMR investigating the mobility of the water in epoxy resulting in the distinction between two type of bonding depending on difference in bond complexity and activation energy. Type I bonding posses the lower activation energy and it is easier to remove from the resin. Type II forms multiple hydrogen bonds with the resin network and thus is harder to remove. According to the authors the first type of bonding is responsible for disrupting inter-chains bonding increasing chain segment mobility and thus acting as a plasticizer. The second type provides a pseudo cross-linking creating bridging between chains. Apicella et al. [2-4] proposed three absorption modes: bulk dissolution of water in polymer network, moisture absorption onto the surface of vacuoles which define the excess of free volume of the glassy structure, hydrogen bonding between polymer hydrophilic groups and water. Xiao et al. [5] using FTIR and NMR also underline the importance of the irreversible changes in the epoxy structure caused by hydrolysis reactions.
Because of the intrinsic effects that water produces on epoxy, physical and mechanical characteristics are found to widely vary with water concentration. Such effects have been pointed out, for instance in [6-10], where, DMA, DSC or TMA analysis have been used to investigate the evolution of T_g, storage and loss modulus with increasing water concentrations. The main results outlined are that, for different epoxies and hardener

combinations, 1% of water mass gain during ageing results in lowering the T_g about 10°C, a loss of 20-40% in storage modulus and 30-40% in tensile strength.
Another important parameter is the coefficient of moisture expansion (CME) which for a given temperature is a function of moisture in the specimen. For an isotropic material, a one dimensional hygric strain ε_z is defined as

$$\varepsilon_z = \beta_m c(x,t) \tag{1}$$

Here $\beta_m(c)$ is the CME, a function of the moisture concentration $c(\boldsymbol{x},t)$ (where $\boldsymbol{x}$ indicates position in the specimen and t is time). This one dimensional equation is realistic when $c(\boldsymbol{x},t)$ and $\beta_m(c)$ are uniform throughout the central part of specimen. Since such experimental conditions are not possible to realize, average parameters are used in Eq. (1). Thus $c(\boldsymbol{x},t)$ should be replaced by an average concentration $\overline{c}(t)$ and the CME of the specimen is assumed uniform, at least away from the specimen's edges, such that $\beta_m(c) \sim \beta_m(\overline{c})$. While different methods have been proposed to experimentally characterise the CME [11, 12], the existing methods present drawbacks regarding their accuracy.
In this work fibre Bragg gratings (FBG) are used for accurate measurements of CME. In addition, traction and relaxation tests on the pure matrix have been performed on specimen at different water content in order to asses the evolution of instantaneous and relaxation moduli. Finally, stress analysis is carried out by accounting for the residual and the moisture induced strains.

Materials

The epoxy under investigation is a mixture of two resins DER330© DER732© and the hardener DEH26© provided by the DOW chemical company. This mixture, in fixed weight proportion of 70:30:10, respectively, have been stirred in vacuum in order to eliminate the presence of bubbles and casted in a specially designed vertical mould that keeps the fiber with the sensor axially aligned. The resulting specimen is a cylinder of 12mm in diameter and a length of 40mm, a single fibre composite (Fig. 1a), and considered as representative composite unit cell. The optical single mode fibre with diameter of 125μm contains a FBG 23mm long. In such configuration, the fibre plays the role of reinforcement and sensor for distributed strains measurement along the fibre direction. More information about specimen preparation and thermal cycles are provided in [13] After processing, specimens are placed in a bath at 50°C containing demineralised water.

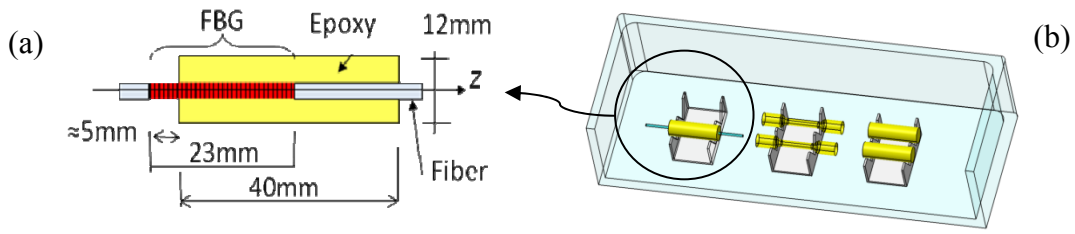

Fig.1: Schematic of specimen geometry (a), section of ageing bath (b).

Control specimens with the same geometry and optical fibres, without FBG, were placed in the same environment and periodically weighted in order to retrieve the absorption curve of this configuration. In the same bath (Fig. 1b) several sets of 5 cylindrical dogbone-like specimens were placed and tested in traction or subjected to relaxation tests into the water using a particular designed bath in order to keep the temperature controlled and to prevent moisture desorption from the specimens. Considering the low speed of diffusion compared to the testing time, additional absorption during the mechanical tests is considered insignificant.

Optical measurements and strains along the FBG

Residual and hygrothermal strains have been monitored using optical low coherence reflectometer [14] and layer peeling technique allowing for the local Bragg wavelength reconstruction. Once the local wavelength is known, with a spatial resolution of less the 20μm, local strains can be calculated. For isothermal conditions, the wavelength change and the strains are related by

$$\frac{\lambda_B(z)-\lambda_{B0}}{\lambda_{B0}} = \left(1-p_e\right)\varepsilon_z(z) \qquad (2)$$

Where the z is the axial direction, p_e is a grating gage factor assumed to be 0.2148, λ_{B0} is the reference Bragg wavelength and $\lambda_B(z)$ is the local Bragg wavelength. Note that the strains are linearly related to the wavelength shift.

Results

Absorption curves

In order to determine the two parameters involved in the water diffusion kinetic trough the resin, i.e., diffusivity and saturation point, the reference and dog-bones like specimens were periodically weighted, using a digital balance with a resolution of 0.01mg, at different intervals of time for an immersion period of approximately one year. The absorption curve from the dog-bones specimens is reported in Fig.2 (solid line) where water gain percentage $w_g\%$ is defined as $w_g\% = \left[\left(W(t)-W(0)\right)/W(0)\right]$ where W are the weights of the specimen at 0 and t times, respectively. Using identification procedure it has been possible to evaluate diffusivity $D \approx 2.04\text{x}10^{-6}$ mm^2/s and the saturation point $s \approx 5.5w_g\%$, as the horizontal tangent at very long time. In fact a pure Fickian diffusive model has been implemented and the two parameters have been varied in order to match the absorption curve experimentally determined. Six representative groups of at least four specimens each, used for mechanical testing, are also indicated in Fig. 2 referring to conditions immediately before testing.

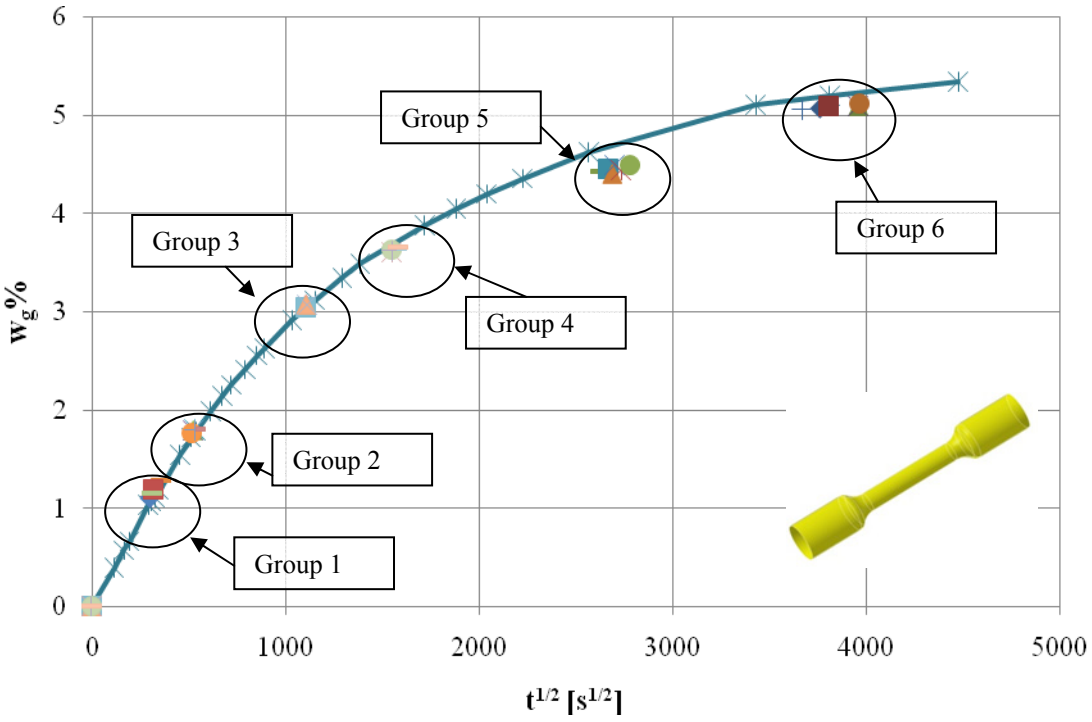

Fig.2: Absorption curve of cylindrical dog-bones specimens (solid line), traction and relaxation specimen weight immediately before testing (encircled points).

Traction tests

In order to establish the influence of water uptake onto Young's modulus, dog bone specimens have been tested: in dry condition at room temperature, in dry condition at 50°C, corresponding to the temperature of the ageing bath and at 50°C but at different percentage of water content corresponding to each one of the 6 groups indicated in Fig. 2. Particular attention was paid to perform tests after achieving thermal equilibrium since relatively high temperature plays an important role in lowering material properties. The specimens were pulled to fracture once the temperature had reached 50°C. Results of these measurements are shown in Fig. 3. In the following these values are referred to as the short term Young's moduli.

Relaxation tests

With the same setup used for traction tests, samples belonging to the afore mentioned six groups, have been subjected to multiple relaxation tests in which four successive relaxations at different strain levels, separated by complete unloading, have been performed so that the first imposed relaxation strain is in the linear elastic region of each particular specimen. Since the material relaxation characteristic times are much shorter than the diffusion phenomenon, only the long term relaxation modulus is measured and used in the modeling. The evolution of this parameter with the amount of moisture content is reported in Fig. 3.

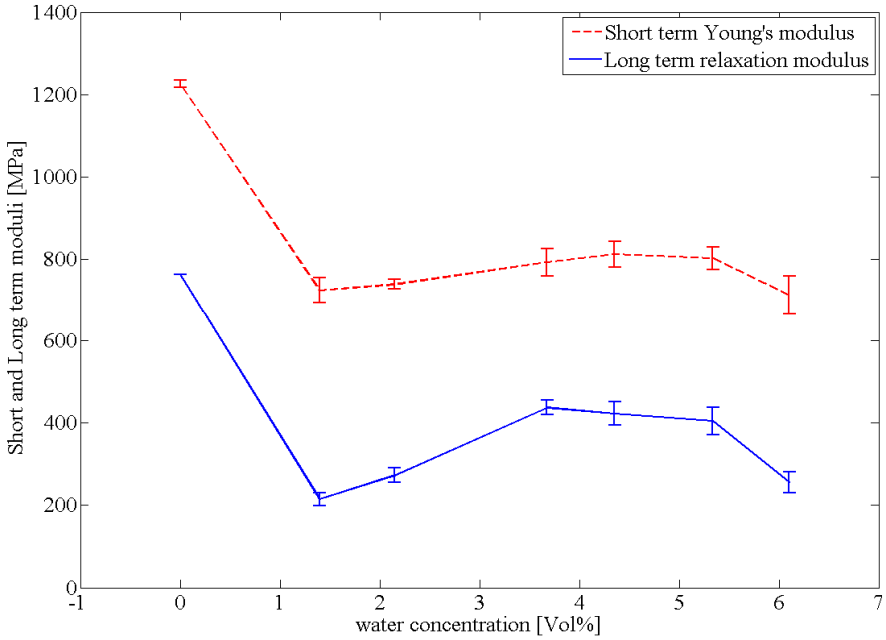

Fig.3: Short and long term moduli evolution against water uptake percentage at 50°C.

Local Bragg evolution during hygrothermal ageing

Local Bragg wavelength evolution during ageing is reported in Fig. 4. Using Eq. (2) the corresponding axial strain distribution is calculated along the FBG sensor. Due to the symmetry of the specimen a similar distribution is assumed from the other end of the specimen. Note the non uniform axial strain, near the entry point of the fibre, which extents up to about a diameter of the specimen. Afterwards, the strains are constant. Considering that inner region of the specimen in iso-strain condition, as evident for the presence of an inner plateau starting approximately at z =16mm, the deformation in this region is attributed only to the epoxy expansion due to water uptake. Interestingly, the initial compressive strains due to post-curing of the epoxy are overcome by the hygric strains and grow significantly into tension after sufficient exposure time.

This strain evolution can be coupled with the experimental absorption curve to obtain the CME $\beta_m(c)$ as follows. Assuming that the glass fibre does not absorb any water, any additional strains in the epoxy at $50^{o}\mathrm{C}$ are due to water. Thus, in the iso-strain region of the specimen Eq. 2 takes the form

$$\frac{\lambda_B(z)-\lambda_{B0}(z)}{\lambda_{B0}(z)} = \left(1-p_e\right)\beta_m(\bar{c})\bar{c}(t) \qquad (3)$$

Where $\bar{c}(t) = \left(\rho_e / \rho_w\right) w_g\%$ in which ρ_e =1.2g/cm^3 and ρ_w =1 g/cm^3 are the densities of epoxy and water, respectively.

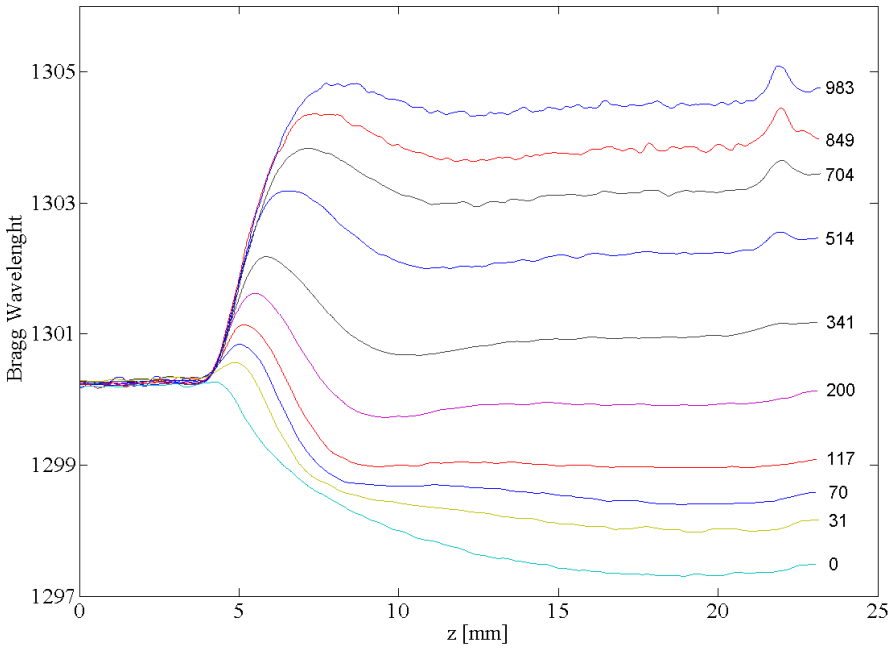

Figure 4: Local Bragg wavelength along the FBG length as a function of immersion time (in hours) shown by the numbers next to the curves.

Using the $\overline{c}(t)$ measurements and the data in Fig. 4 at z = 20mm, $\lambda_{B0}(z=20mm)=1297.13\,\text{nm}$, the left hand side of (3) is divided by $(1-p_e)$ and its values are plotted against $\overline{c}(t)$ in Fig. 5. Note that, $\beta_m(\overline{c})$ (the slope of the curve) is not constant. However, the data can be approximated by two straight lines, at relatively low and relatively high values of $\overline{c}(t)$ with corresponding ranges of slopes of $\beta_m(\overline{c}) \approx 0.09$ to 0.13 and from 0.22 to 0.24. Similar results are shown in [15]. Note that the initial strain response in Fig. 5 is assumed to be due to pores filled by water with less effects on hygric strains [16] and the latter is a reasonable value for an epoxy at 50^{o}C and for epoxy based composites [11, 17].

Modeling

Extensive use of numerical modelling of the single fibre composite has been employed to design the experiment and to compare hygrothermally induced strains with experimental data; for reasons of geometry symmetry only one half of the specimen in axial symmetric formulation has been studied. In particular the following models have been implemented using the commercial code ABAQUS©:

1. A transient heat transfer model to estimate the time to thermal equilibrium after specimen immersion into the water bath at 50°C

$$\frac{\partial T}{\partial t}=\frac{k}{\rho c_p}\nabla^2 T \qquad (4)$$

Where ρ is the density of the materials (ρ_{glass}=2.54 gr/cm^3 , ρ_{epoxy}=1.2gr/cm^3), k is the thermal conductivity (k_{glass}=1.32Wm^{-1} K^{-1} ,k_{epoxy}=0.2Wm^{-1}K^{-1}) and c_p is the specific heat capacity(c_{pglass}=0.81J gr^{-1}K^{-1}, c_{pepoxy}=1 Jgr^{-1}K^{-1}).

As boundary conditions a natural convection in water at the external surface of the specimen was imposed, in particular the input heat flux $q=h_{ext}(T-T_{ext})$, was calculated using natural convection coefficient h_{ext}= 20Wm^{-2}K.

The time necessary to establish thermal equilibrium has been considered the one at which the inner zone of the specimens reaches 99% of the external imposed temperature corresponding to ≈ 15 min.

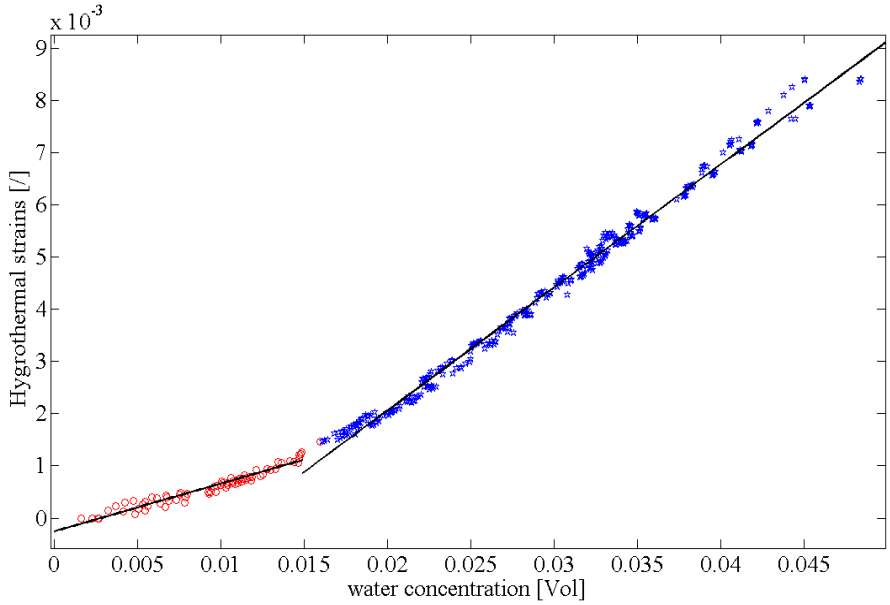

Fig. 5: Evolution of axial strains for 4 specimens at z = 20mm as function of water concentration. The slope of the interpolation is defined as the coefficient of moisture expansion.

2. A Fickian moisture diffusion model to identify diffusion parameters D and s.

   In this model normalized concentration $c^*(\boldsymbol{x},t) = c(\boldsymbol{x},t)/s$ is defined. Thus, the following conditions are imposed at time $t = 0$, $c^* = 0$ in the specimen volume while $c^* = 1$ at the external boundary at all times

$$\frac{\partial c^*}{\partial t} = D\nabla^2 c^* \tag{5}$$

3. A coupled hygromechanical model in order to investigate the influence of the non uniform concentration field on the stress field induced by moisture induced expansion. In this model eq. 5 is solved simultaneously with

$$\sigma = C\left(\varepsilon + \beta_m s c^* I\right) \tag{6}$$

Where ε and σ are the strain and stress tensors and $\boldsymbol{C}$ and $\boldsymbol{I}$ are the elasticity and identity tensors. The CME $\beta_m(\bar{c})$ is taken as the secant value from the whole set of the experimental data in Fig. 5.

The experimental data on the material properties are used in the elastic model in the region of the specimen with the uniform strain. In particular, in the first model the short term Young modulus measured with traction tests has been used (Sim. 1) and in the second one, the long term modulus retrieved by the relaxation tests has been implemented as modulus of the epoxy in the simulations (Sim. 2). In addition an average value of the long term modulus (averaged using the 2nd to last values, Fig. 6) is used (Sim. 2b). The results of the simulation and the experimental data are shown in Fig. 6 for about 1700 hrs of immersion.

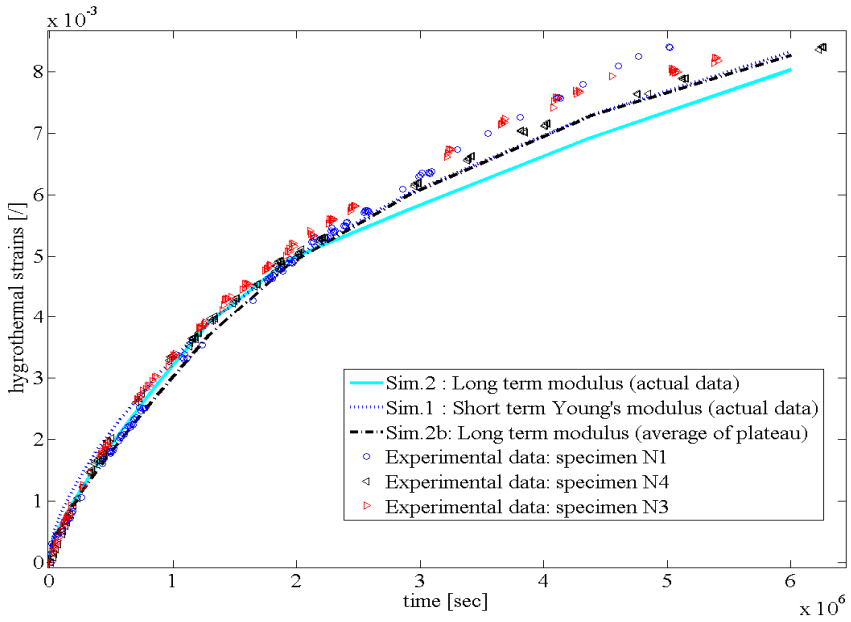

Fig. 6: Axial strain evolution in time, experimental data from 3 specimens and FE predictions.

Discussion

The common characteristic between traction and relaxation tests reported in Fig. 3, i.e., the tendency to a recovery in both the short and long term moduli has been already reported in [18] for similar material where was noticed in the evolution of the storage modulus even though it was not explained. It is interesting that this difference accentuate in the long term modulus (Fig. 3).

Good reproducibility in the determination of the CME is evident in Fig. 5, especially up until ~3.5% of water absorption, were data of 4 specimens are reported demonstrating the high accuracy of the method. Differences appear between the data from the different specimens, at relatively higher moisture absorption, and are attributed to experimental errors coming from the measurements of water absorption of the control specimens and wavelength measurements during the immersion.

In the literature a constant value of CME is usually reported for a given temperature [11]. The results of this study (Fig. 5) and the one reported earlier [15] show that a single value of CME is not adequate to model the evolution of the hygric strains.

When the variation of the CME as a function of moisture is used in the simulations (Fig. 5), the experimental data and the results of the simulation, shown in Fig. 6, are in good agreement. Note that the differences are much smaller in the first half of the ageing process and grow to about 13% at the end of the experiment. One reason for these differences may be that a single set of data was used in the evaluation of CME and not an averaged value on all the specimens. It should be noted also that the CME reported in [15] was smaller by 15%. Such a difference is attributed to a smaller range of absorption used in [15].

Regarding the influence of the Young modulus on the simulation results, it is seen that for the most part, the data are in good agreement independently of what modulus is used. The agreement of the experimental data and the simulations is not as good after $3x10^6$s of immersion which corresponds to (~3.8% vol of moisture). The source for this behaviour is not clear and additional research is required to elucidate it.

Conclusion

FBGs have demonstrated to be an accurate tool in determining the coefficient of moisture expansion ,that result to be function of average moisture concentration, and in monitoring strain development during ageing of polymer materials. As pointed out by numerical modelling this parameter plays a predominant role in strain development during ageing, never the less, since the exposure covers several months, materials properties evolution with water content holds importance in particular with respect to the relaxed conditions.

ACKNOWLEDGEMENTS

The authors wish to acknowledge the financial support from the Swiss National Science Foundation, grant N^o 113710.

References

1. *Zhou, J. and J.P. Lucas, Hygrothermal effects of epoxy resin. Part I: the nature of water in epoxy. Polymer, 1999.* ***40****(20): p. 5505-5512.*
2. *Apicella, A., L. Nicolais, G. Astarita, and E. Drioli, Effect of thermal history on water sorption, elastic properties and the glass transition of epoxy resins. Polymer, 1979.* ***20****(9): p. 1143-1148.*
3. *Apicella, A., L. Nicolais, G. Astarita, and E. Drioli, Hygrothermal history dependence of equilibrium moisture sorption in epoxy resins. Polymer, 1981.* ***22****(8): p. 1064-1067.*
4. *Apicella, A., R. Tessieri, and C. de Cataldis, Sorption modes of water in glassy epoxies. Journal of Membrane Science, 1984.* ***18****: p. 211-225.*

5. *Xiao G. Z. , Delamar M., and S. M., Irreversible interactions between water and DGEBA/DDA epoxy resin during hygrothermal aging. Journal of Applied Polymer Science, 1997.* ***65****(3): p. 449-458.*
6. *Ellis T. S. and K.F. E., Interaction of epoxy resins with water: the depression of glass transition temperature. Polymer, 1984.* ***25****(5): p. 664-669.*
7. *Zhou, J. and J.P. Lucas, Hygrothermal effects of epoxy resin. Part II: variations of glass transition temperature. Polymer, 1999.* ***40****(20): p. 5513-5522.*
8. *W. J. Mikols, J. C. Seferis, A. Apicella, and L. Nicolais., Evaluation of structural changes in epoxy systems by moisture sorption-desorption and dynamic mechanical studies. Polymer Composites, 1982.* ***3****(3): p. 118-124.*
9. *Nogueira P., Ramirez C, Torres A, Abad M. J., Cano J, Lopez J, Lopez-Bueno I, and B. L., Effect of water sorption on the structure and mechanical properties of an epoxy resin system. Journal of Applied Polymer Science, 2001.* ***80****(1): p. 71-80.*
10. *Papanicolaou G. C., Kosmidou Th V., Vatalis A. S., and Delides C. G., Water absorption mechanism and some anomalous effects on the mechanical and viscoelastic behavior of an epoxy system. Journal of Applied Polymer Science, 2006.* ***99****(4): p. 1328-1339.*
11. *Daniel M.Isaac and I. Ori, Engineering Mechanics of Composite Materials. 2006: Oxford.*
12. *Wong, E.H., R. Rajoo, S.W. Koh, and T.B. Lim, The Mechanics and Impact of Hygroscopic Swelling of Polymeric Materials in Electronic Packaging. Journal of Electronic Packaging, 2002.* ***124****(2): p. 122-126.*
13. *Lai, M., J. Botsis, D. Coric, and J. Cugnoni. On the degree of conversion and coefficient of thermal expansion of a single fiber composite using a FBG sensor. in 4th International Conference on Times of Polymers TOP and Composites. 2008. Ischia, ITALY: Amer Inst Physics.*
14. *Giaccari P., Dunkel G. R., Humbert L., Botsis J., Limberger H. G., and S. R.P., On a direct determination of non-uniform internal strain fields using fibre Bragg gratings. Smart Materials and Structures, 2005(14): p. 127.*
15. *Karalekas, D., J. Cugnoni, and J. Botsis, Monitoring of hygrothermal ageing effects in an epoxy resin using FBG sensor: A methodological study. Composites Science and Technology, 2009.* ***69****(3-4): p. 507-514.*
16. *Whitney J.M., Daniel I.M., and P. R.B., Experimental Mechanics of fiber Reinforced composite Materials, ed. S.M. No.4. 1984.*
17. *Lin, Y., Investigation of the Moisture-Desorption Characteristics of Epoxy Resin. Journal of Polymer Research, 2006.* ***13****(5): p. 369-374.*
18. *Nunez, L., M. Villanueva, F. Fraga, and M.R. Nunez, Influence of water absorption on the mechanical properties of a DGEBA (n = 0)/1, 2 DCH epoxy system. Journal of Applied Polymer Science, 1999.* ***74****(2): p. 353-358.*